Observational Study

Medicine

OPEN

Impact of distinct insulin index on neoadjuvant treatment of breast cancer

A clinical retrospective study

Yi Zeng, MM[a,*]

Abstracts

A combination of glucose and lipid metabolism, insulin resistance (IR) is correlated with the outcome of neoadjuvant treatment (NAT) for breast cancer. The purpose of this research sought to explore how IR affects breast cancer patients' reactions after NAT. We gathered 132 individuals with breast cancer who had surgery after NAT. Continuous values were analyzed using the Wilcoxon (Mann–Whitney) test and independent samples *t* test; pathological complete response (PCR)-related independent influencing factors were investigated using the binary logistic regression model; and the predictive value of each index on the effectiveness of NAT was assessed using subject work characteristics (receiver operating characteristic) curves. Compared with the non-PCR group, the PCR group's IR levels were lower. Baseline IR levels and NAT effectiveness did not significantly correlate, according to multifactorial logistic analysis ($P > .05$). Nevertheless, there was a negative correlation ($P < .05$) between PCR and total cholesterol (TC)/high-density lipoprotein (HDL) and MetS-IR levels following NAT. According to the receiver operating characteristic curve prediction model, TC/HDL had a greater predictive value than MetS-IR. Dynamic IR indicators (ΔTC/HDL and ΔMetS-IR) demonstrate predictive value for NAT response in breast cancer, mechanistically linked to lipid metabolism reprogramming and immunosuppressive tumor microenvironment. Future multicenter studies should validate optimal thresholds and investigate combined metabolic-immune targeted therapeutic strategies.

Abbreviations: 95% CI = 95% confidence interval, A+T = anthracycline + paclitaxel, BMI = body mass index, ER = hormone receptor, FBG = fasting blood glucose, HDL-C = high-density lipoprotein cholesterol, HER2 = human epidermal growth factor receptor 2, IR = insulin resistance, LDL-C = low-density lipoprotein cholesterol, NAT = neoadjuvant therapy, PCR = pathological complete response, T = paclitaxel, TC = total cholesterol, TG = triglycerides.

Keywords: breast cancer, insulin resistance, neoadjuvant therapy, pathological complete response

1. Introduction

In the treatment of breast cancer, neoadjuvant therapy (NAT) has been increasing in emphasis.[1] It can accomplish the objective of monitoring treatment sensitivity, decreasing tumor size, lowering clinical stage, and enabling more patients to satisfy the criteria for breast-conserving surgery.[2] Compared to adjuvant chemotherapy, more patients in the EBCTCG trial had breast-conserving treatment with NAT, and neither overall survival (OS) nor distant recurrence rates differed significantly.[3] Neoadjuvant and adjuvant treatment did not vary in disease-free survival as well as OS, according to the NSABP B-18 and B-20 investigations.[2,4] Nonetheless, disease-free survival and OS were greater in those who obtained pathological complete response (PCR) following NAT.[5–7] According to CTNTNeoBC, there was a strong correlation between PCR and both OS and EFS.[8] Consequently, NAT patients' prognosis may be enhanced by early detection and PCR rate improvement.

Reduced insulin signaling in response to blood glucose levels causes insulin resistance (IR), which can result in anomalies in the body's lipid and blood glucose metabolism. According to several theories, IR raises the chance of getting cancer.[9] IR raises the risk of mortality and recurrence while decreasing the PCR rate in patients.[10,11] Consequently, it can be wise to keep an eye on and reduce IR. Thus, keeping an eye on and lowering IR might contribute to higher PCR rates. Alternative scoring indices, including total cholesterol (TC)/high-density lipoprotein

The authors have no funding and conflicts of interest to disclose.

The datasets generated during and/or analyzed during the current study are available from the corresponding author upon reasonable request.

This research was conducted in accordance with the standards set out in the Declaration of Helsinki. This study was approved by the Ethics Review Committee of the Affiliated Huizhou Hospital, Guangzhou Medical University (Research Approval Number: 2024-KY-127-01). Based on the retrospective nature of the study, the need for written informed consent was waived by the Ethics Review Committee of the Affiliated Huizhou Hospital, Guangzhou Medical University. However, all participants had the opportunity to opt-out on the homepage of the Ethics Review Committee of the Affiliated Huizhou Hospital, Guangzhou Medical University.

[a] *Department of Breast Surgery, The Affiliated Huizhou Hospital, Guangzhou Medical University, Huizhou, Guangdong, China.*

[*] *Correspondence: Yi Zeng, Department of Breast Surgery, The Affiliated Huizhou Hospital, Guangzhou Medical University, No.1 Xuebei Road, Huizhou, Guangdong, 516000 China (e-mail: 568156441@qq.com).*

How to cite this article: Zeng Y. Impact of distinct insulin index on neoadjuvant treatment of breast cancer: A clinical retrospective study. Medicine 2025;104:19(e42356).

Received: 4 December 2024 / Received in final form: 2 April 2025 / Accepted: 18 April 2025

http://dx.doi.org/10.1097/MD.0000000000042356

(HDL), triglycerides (TG)/HDL, triglyceride glucose (TyG), and MetS-IR, are accessible as trustworthy biochemical markers for evaluating IR; nevertheless, conventional hyperinsulinemic-euglycemic clamp (HIEC) sampling is time-consuming and expensive.[12–14] The previously described IR score indices have been shown to be substantially correlated with the prognosis of breast cancer in a number of large cohort studies, such as REACTION.[15,16]

In summary, we think that NAT effectiveness in breast cancer may be accurately predicted using the IR score index. Additionally, it is possible to directly acquire the scoring-related indices from peripheral venous blood, which offers the benefits of easy sample and reduced expense. To serve as a guide for clinical diagnosis and treatment, this study intends to investigate the predictive value of several IR score indices on the effectiveness of NAT in patients with breast cancer.

2. Methods

2.1. Patient selection

This study evaluates patients who were diagnosed with breast cancer and had surgery after NAT (with or without anti-HER2 therapy) at Huizhou City's Third People's Hospital from January 1, 2017 to September 31, 2024.

Inclusion criteria for the study included women between the ages of 18 to 80 years; undergoing surgery after NAT, which included modified radical, breast-conserving, and subcutaneous adenotonsillectomy; invasive breast cancer with clear hormone receptor (ER), progesterone receptors (PR), HER2, and Ki-67% status; no history of malignancy in other organs or systems; stage I–III breast cancer (refer to American Joint Committee on Cancer [AJCC] 8th edition)

Exclusion criteria included neoadjuvant targeted therapy or endocrine therapy only, stage 0 or IV breast cancer (refer to AJCC 8th edition), incomplete chemotherapy cycle, concomitant malignancy of other organs or systems, missing pathologic data, disease progression during NAT, and no surgical treatment after NAT.

2.2. Information collection and evaluated parameters

Clinical and pathologic data of patients were collected, including age, height, weight, body mass index (BMI), menstrual status, history of hypertension, puncture pathology results, surgical procedure, postoperative pathology results, fasting blood glucose (FBG), fasting TC, fasting TG, fasting HDL-C, and fasting low-density lipoprotein (LDL-C).

According to the IR assessment formula, fasting TyG index = LN[TG (mg/dL)*FBG (mg/dL)/2], MetS-IR = LN[2*FBG (mg/dL) + TC (mg/dL)*BMI)/Ln(LDL (mg/dL)], TG-to-HDL ratio = TC (mg/dL)/HDL (mg/dL), and TG-to-HDL ratio = TG (mg/dL)/HDL (mg/dL).

TNM staging was determined according to the 8th edition AJCC criteria. All pathologic diagnoses, immunohistochemical data, and PCR status were obtained from our institution's Diagnostic Pathology Center. Referring to the Guidelines of Chinese Society of Clinical Oncology (2024 CSCO), the criteria for HR positivity were ER ≥ 1% or PR ≥ 1%, and the criteria for HER2 positivity were 3+ or 2+ on IHC, and≥2+ on HER2 amplification (HER2/CEP17) by fluorescence in situ hybridization. In this study, Ki-67% > 30% was defined as high expression of Ki-67, and ≤30% was defined as low expression of Ki-67. According to ER, PR, and HER2 expression, patients were categorized into 4 groups: HR(+)/HER2(−), HR(−)/HER2(−), HR(−)/HER2(+), and HR(+)/HER2(+).

The NAT regimen consisted of anthracycline-based combined with a zithromax (group A + T) and a zithromax combined with other drugs based on guideline recommendations (group T), with or without anti-HER2 therapy. All patients underwent imaging every 2 cycles during treatment to assess clinical efficacy. All patients underwent surgery after NAT. Post-NAT PCR pathology was evaluated using the criteria ypT0ypN0, defined as the absence of residual tumor cells in the primary tumor (breast PCR) and axillary lymph nodes (axillary PCR) after neoadjuvant chemotherapy.

2.3. Statistical analysis

The statistical program SPSS 29.0 (IBM [International Business Machines Corporation], Armonk) was used to examine the data. The mean ± standard deviation ($\bar{X} \pm s$) was used to describe quantitative data that satisfied the normal distribution, and the independent samples *t* test was used to compare groups. M (P25–P75) was used to represent quantitative data that did not fit the normal distribution, and the Wilcoxon (Mann–Whitney) test was used to compare groups. The symbol for qualitative data is n (%). Binary logistic regression was used for multifactor analysis, and statistically significant indicators from the univariate analysis were incorporated into the multifactor analysis model.

The subject's work characteristics (receiver operating characteristic [ROC]) curve was used to assess each indicator's predictive value for NAT effectiveness, and Jordan's index was used to identify the ideal cutoff value. When $P < .05$, differences were deemed statistically significant.

3. Results

3.1. Comparison of clinical case characteristics

The research involved 132 patients in total. There were 78 non-PCR instances and 54 post-NAT up to PCR cases. One hundred patients were over 40, while 32 patients were under 50. In this study, BMI was divided into 3 groups: ≥28 (n = 15), 24–27.99 (n = 41), and < 24 (n = 76). Seventy did not have hypertension, whereas 62 did. Clinical stages IIa–IIb were present in 68 individuals, while stage IIIa–IIIc was present in 64 patients. The cases were grouped by immunohistochemical type: 42 HR+/HER2 cases, 28 HR−/HER2 cases, 34 HR+/HER2+ cases, and 29 HR−/HER2+ cases. There were 97 instances with a high Ki-67 level and 35 cases with a low Ki-67 level (Fig. 1). The PCR group had fewer patients with hypertension and lower BMI values than the non-PCR group. Additionally, the comparison of the subtype subgroups showed a notable difference. However, there was no correlation between Ki-67, clinical stage, age, or menstruation (Table 1).

In the comparison of baseline lipid metabolic indicators, overall FBG, all lipids, and IR values were lower in the PCR group than in the non-PCR group, according to statistical statistics. Significant variations were seen in TG, LDL, TG/HDL, and TyG among them. TG (0.97 [0.76–1.40] vs 1.24 [0.89–1.75], $P = .018$), LDL (2.88 ± 0.74 vs 3.15 ± 0.87, $P = .033$), TG/HDL (1.47 [1.16–2.29] vs 2.12 [1.36–3.32], $P = .034$), TyG/HDL (1.47 [1.16–2.29] vs 2.12 [1.36–3.32], $P = .034$), and TyG (8.49 ± 0.65 vs 8.67 ± 0.51, $P = .040$) were all significantly different from the non-PCR group (Table 2 and Fig. 2).

Significant variations in TG/HDL and TyG between the PCR and non-PCR groups were indicated by univariate analysis (Table 2 and Fig. 2). After controlling for hypertension, subtype, BMI, and LDL, multifactorial analysis revealed no discernible change in TG/HDL (odds ratio [OR] = 0.997, 95% confidence interval [CI]: [0.841–1.183], $P = .976$) or TyG (OR = 0.940, 95% CI: [0.455–1.146], $P = .869$) (Table 3). According to the findings, there was no discernible relationship between baseline TG/HDL and TyG and the effectiveness of NAT therapy.

Relevant NAT, the following metabolic indices were established: Delta-FBG (dFBG), Delta-Lipid (dLipid), and Delta-IR

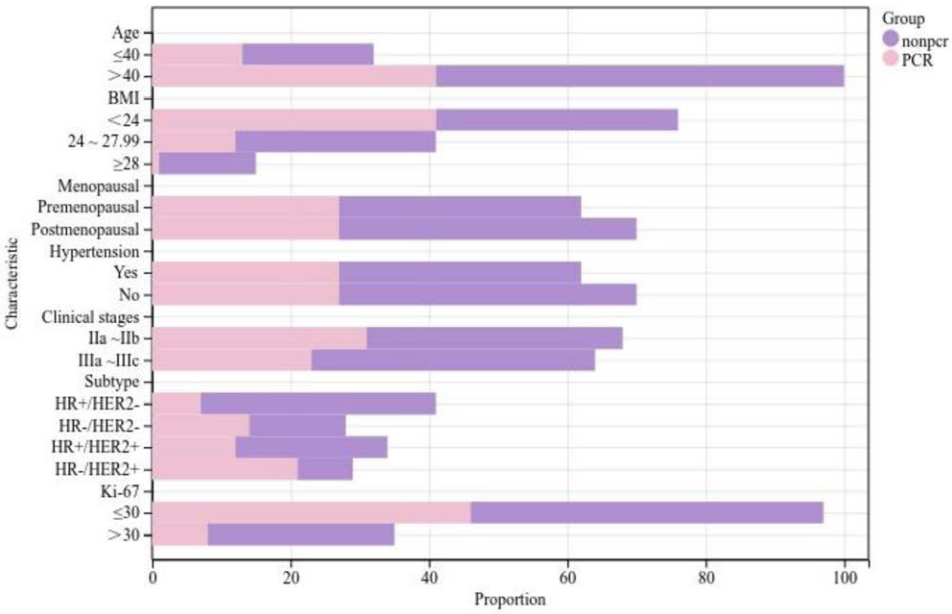

Figure 1. Distribution of general clinical and pathologic features. BMI = body mass index, HR = hormone receptor, HER2 = human epidermal growth factor receptor 2.

Table 1

Univariate analysis of general clinical and pathological characteristics with pathological complete remission.

	Pathological complete remission				
Characteristic	**PCR**	**Non-PCR**	**OR**	**95% CI**	***P* value**
Age (years), cases (%)					
≤40	13 (40.6)	19 (59.4)	Ref.	Ref.	Ref.
>40	41 (41.0)	59 (59.0)	0.985	0.438–2.214	.970
BMI (kg²/m²), cases (%)					
<24	41 (53.9)	35 (46.1)	Ref.	Ref.	Ref.
24~27.99	12 (29.2)	29 (70.8)	2.831	1.259–6.363	**.012**
≥28	1 (6.6)	14 (93.4)	16.400	2.052–131.049	**.008**
Menopausal					
Premenopausal	27 (43.5)	35 (56.5)	Ref.	Ref.	Ref.
Postmenopausal	27 (38.5)	43 (61.5)	1.229	0.613–2.463	.562
Hypertension, cases (%)					
Yes	27 (43.5)	35 (56.5)	Ref.	Ref.	Ref.
No	27 (38.5)	43 (61.5)	0.363	0.135–0.975	**.044**
Clinical stages, cases (%)					
IIa~IIb	31 (45.5)	37 (48.5)	Ref.	Ref.	Ref.
IIIa~IIIc	23 (35.9)	41 (64.1)	1.494	0.742–3.004	.261
Subtype, cases (%)					
HR+/HER2–	7 (17.0)	34 (83)	Ref.	Ref.	Ref.
HR–/HER2–	14 (50.0)	14 (50.0)	0.206	0.069–0.619	**.005**
HR+/HER2+	12 (35.2)	22 (64.8)	0.377	0.129–1.106	.076
HR–/HER2+	21 (72.4)	8 (17.6)	0.078	0.025–0.248	**<.001**
Ki-67, cases (%)					
≤30	46 (47.4)	51 (52.6)	Ref.	Ref.	Ref.
>30	8 (22.8)	27 (77.3)	0.846	0.380–1.883	.681

Bold value indicates statistically significant differences.

BMI = body mass index, CI = confidence interval, HER2 = human epidermal growth factor receptor 2, HR = hormone receptor, OR = odds ratio, PCR = pathological complete response.

(dIR). As a whole, the non-PCR group had greater FBG, cholesterol, and IR levels than the PCR group (Fig. 3). The PCR group had lower dTC (4.57 ± 0.72 vs 5.25 ± 1.07 $P < .001$), dLDL (2.89 ± 0.66 vs 3.20 ± 1.03 $P = .001$), dTC/HDL (3.35 (2.86,3.98) vs 4.05 (3.37,5.15) $P < .001$), dTLC/HDL (3.35 (2.86,3.98) vs 0.001), dTyG (8.72 ± 0.59 vs 8.89 ± 0.49 $P = .041$), and insulin resistance metabolic score following neoadjuvant chemotherapy (dMetS-IR) (2.14 ± 0.15 vs 2.20 ± 0.19 $P = .018$) that were significantly different from the non-PCR group. Regimens, dFBG, dTG, and dHDL, did not significantly correlate ($P > .05$) (Table 4).

According to univariate analysis, there was a substantial correlation between PCR and dTC/HDL, TG/HDL, TyG, and MetS-IR (Table 4 and Fig. 3). Multivariate logistic analysis showed that dTC/HDL ($P = .018$) and dMetS-IR ($P = .034$) were significantly correlated with PCR and both of them were

Table 2

Univariate analysis of baseline metabolic level and pathological complete remission.

Indicators	Total (N = 132)	PCR group (n = 54)	Non-PCR group (n = 78)	*P* value
FBG (mmol/L), M (P25–P75)	5.49 (5.07–5.96)	5.42 (5.04–5–79)	5.51 (5.11–6.08)	.449
TC (mmol/L), M (P25–P75)	4.65 (4.23–5.31)	4.54 (4.18–5.21)	4.72 (4.30–5.42)	.122
TG (mmol/L), M (P25–P75)	1.15 (0.82–1.57)	0.97 (0.76–1.40)	1.24 (0.89–1.75)	**.018**
HDL (mmol/L), M (P25–P75)	1.38 (1.17–1.74)	1.37 (1.20–1.74)	1.40 (1.14–1.76)	.753
LDL (mmol/L), M ($\bar{X} \pm s$)	3.03 ± 0.82	2.88 ± 0.74	3.15 ± 0.87	**.033**
TC/HDL, M (P25–P75)	3.41 (2.77–3.90)	3.32 (2.85–3.70)	3.44 (2.72–4.21)	.175
TG/HDL, M (P25–P75)	1.82 (1.23–2.81)	1.47 (1.16–2.29)	2.12 (1.36–3.32)	**.034**
TyG, $\bar{X} \pm s$	8.60 ± 0.58	8.49 ± 0.65	8.67 ± 0.51	**.040**
MetS-IR, M (P25–P75)	2.22 (2.10–2.34)	2.18 (2.09–2.29)	2.26 (2.11–2.37)	.093

Bold value indicates statistically significant differences.

FBG = fasting blood glucose, HDL-C = high-density lipoprotein cholesterol, LDL-C = low-density lipoprotein cholesterol, M = median, PCR = pathological complete response, TC = total cholesterol, TG = triglycerides, $\bar{X} \pm s$ = mean ± standard deviation.

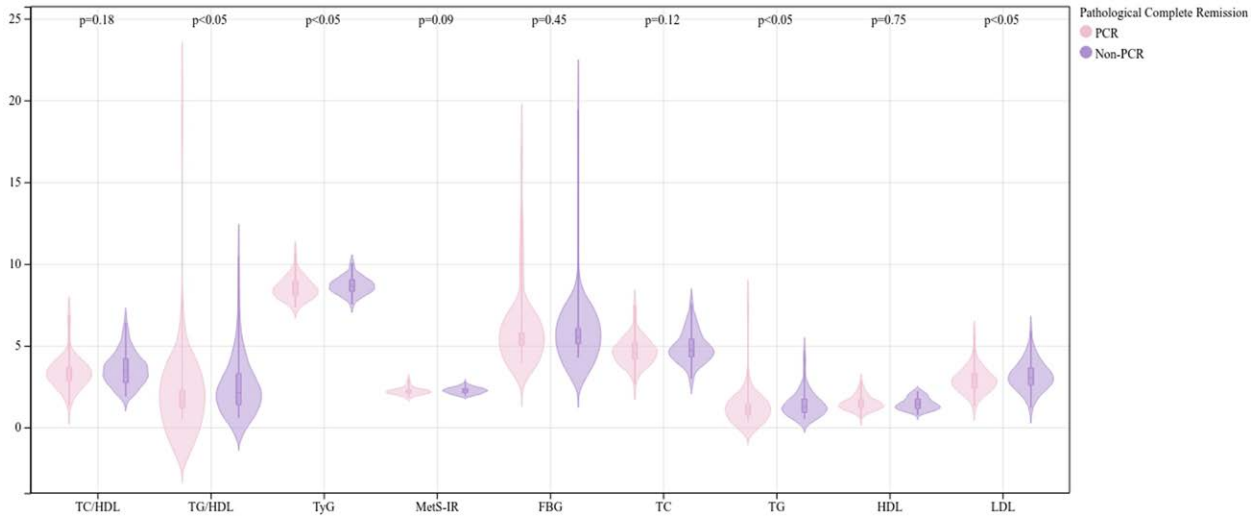

Figure 2. Univariate analysis of baseline metabolic level and PCR. FBG = fasting blood glucose, HDL-C = high-density lipoprotein cholesterol, LDL-C = low-density lipoprotein cholesterol, PCR = pathological complete response, TC = total cholesterol, TG = triglycerides.

Table 3

Multifactorial analysis of insulin resistance and pathological complete remission.

						OR 95% CI	
Indicators	***B***	**SE**	**Wald**	***P* value**	**OR**	**Lower**	**Upper**
(a)							
TG/HDL	−0.003	0.087	0.001	.976	0.997	0.841	1.183
Hypertension	−1.006	0.586	2.947	.086	0.366	0.116	1.153
Subtype	−0.658	0.190	12.051	**<.001**	0.518	0.357	0.751
BMI	0.940	0.348	7.303	**.007**	2.559	1.295	5.060
LDL	0.390	0.276	1.991	.158	1.477	0.859	2.537
(b)							
TyG	−0.061	0.371	0.027	.869	0.940	0.455	1.946
Hypertension	−1.033	0.610	2.871	.090	0.356	0.108	1.176
Subtype	−0.661	0.19	12.052	**<.001**	0.516	0.355	0.750
BMI	0.948	0.351	7.304	**.007**	2.581	1.298	5.133
LDL	0.397	0.279	2.014	.156	1.487	0.860	2.571

Bold value indicates statistically significant differences.

BMI = body mass index, CI = confidence interval, HDL-C = high-density lipoprotein cholesterol, LDL-C = low-density lipoprotein cholesterol, OR = odds ratio, TG = triglycerides, TyG = triglyceride glucose.

negatively correlated with PCR rate after controlling for baseline clinicopathologic characteristics such as BMI, hypertension, subtype, dTC, and dLDL. This suggests that dTC/HDL and dMetS-IR were independent influences on the treatment effect of NAT (Table 5).

A ROC prediction model was developed to investigate the impact of dTC/HDL and dMetS-IR on the therapeutic effect of NAT (Fig. 4). The results of the investigation showed that the TC/HDL area under curve (AUC) was 0.700, the sensitivity was 0.920, the specificity was 0.660, and the Yoden Index was

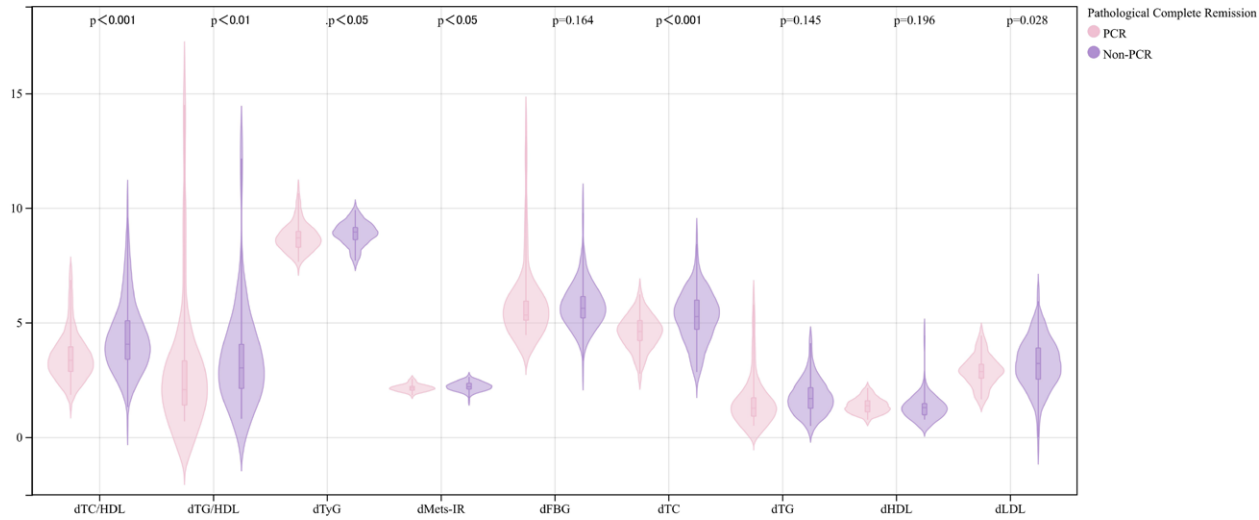

Figure 3. Univariate analysis of delta-metabolism level and PCR. FBG = fasting blood glucose, HDL-C = high-density lipoprotein cholesterol, LDL-C = low-density lipoprotein cholesterol, PCR = pathological complete response, TC = total cholesterol, TG = triglycerides.

Table 4

Univariate analysis of delta-metabolism level and pathological complete remission.

Indicators	Total (N = 132)	PCR group (n = 54)	Non-PCR group (n = 78)	*P* value
dFBG (mmol/L), M (P25–P75))	5.59 (5.14–6.01)	5.33 (5.08–5.95)	5.62 (5.19–6.16)	.164
dTC (mmol/L), M ($\bar{X} \pm s$)	4.97 ± 0.99	4.57 ± 0.72	5.25 ± 1.07	**<.001**
dTG (mmol/L), M ($\bar{X} \pm s$)	1.67 ± 0.89	1.57 ± 1.07	1.74 ± 0.74	.145
dHDL (mmol/L), M ($\bar{X} \pm s$)	1.33 ± 0.43	1.37 ± 0.32	1.30 ± 0.49	.196
dLDL (mmol/L), M ($\bar{X} \pm s$)	3.08 ± 0.91	2.89 ± 0.66	3.20 ± 1.03	**.028**
dTC/HDL, M (P25–P75))	3.65 (3.08–4.44)	3.35 (2.86–3.98)	4.05 (3.37–5.15)	**<.001**
dTG/HDL, M (P25–P75)	2.75 (1.69–3.74)	2.07 (1.38–3.41)	4.05 (3.38–5.14)	**.006**
dTyG, M ($\bar{X} \pm s$)	8.82 ± 0.54	8.72 ± 0.59	8.89 ± 0.49	**.041**
dMetS-IR, M ($\bar{X} \pm s$)	2.18 ± 0.17	2.14 ± 0.15	2.20 ± 0.19	**.018**
Regimens				.079
A + T	85 (64.4%)	29 (53.7%)	56 (71.7%)	
T	47 (35.6%)	25 (46.3%)	22 (28.3%)	

Bold value indicates statistically significant differences.

FBG = fasting blood glucose, HDL-C = high-density lipoprotein cholesterol, LDL-C = low-density lipoprotein cholesterol, M = median, PCR = pathological complete response, TC = total cholesterol, TG = triglycerides, TyG = triglyceride glucose, $\bar{X} \pm s$ = mean ± standard deviation.

0.340. The ROC prediction model was developed using the following metrics: MetS-IR AUC = 0.610, sensitivity = 0.474, specificity = 0.767, and Yoden Index = 0.237.

While the 2 clinical prediction models were compared, it was shown that TC/HDL had a higher predictive power than MetS-IR. To sum up, the IR formula for TC/HDL may be a more accurate indicator of NAT efficacy (Fig. 4).

4. Discussion

IR, a central mechanism underlying glucose and lipid metabolism dysregulation, has been conclusively linked to the pathogenesis of various metabolic disorders.[9] This study investigates the predictive value of IR-associated surrogate indices (e.g., TC/HDL ratio, MetS-IR) for therapeutic outcomes in breast cancer patients undergoing NAT. While IR correlates with poor prognosis and reduced NAT sensitivity in breast cancer,[10] current research predominantly focuses on validating these indices for cancer risk assessment.[12–14] To address the limitations of traditional IR measurements, such as the HIEC, which involves complex protocols and high costs, we conducted a retrospective analysis of 132 NAT-treated breast cancer patients. Our aim was to develop an economic and accessible predictive model using novel metabolic parameters, thereby providing clinicians with a practical tool for treatment response evaluation. To address the limitations of traditional IR measurements, such as the HIEC, which involves complex protocols and high costs, we conducted a retrospective analysis of 132 NAT-treated breast cancer patients. Our aim was to develop an economic and accessible predictive model using novel metabolic parameters, thereby providing clinicians with a practical tool for treatment response evaluation.

This study pioneers the systematic evaluation of dynamic IR evolution during NAT and its correlation with PCR rates, overcoming the limitations of prior studies that focused solely on baseline metabolic profiles. While Szablewski et al[9] and Tong et al.[10] previously reported associations between homeostatic model assessment of insulin resistance and breast cancer prognosis, their conclusions remain contentious due to the exclusion of metabolic fluctuations during treatment. Our analysis revealed no significant correlation between baseline TC/HDL ratio (OR = 1.12, $P = .08$) or MetS-IR (OR = 1.09, $P = .11$) and PCR. In contrast, dynamic post-NAT indices – ΔTC/HDL (OR = 2.34, $P < .001$) and ΔMetS-IR (OR = 2.18, $P = .002$) – demonstrated robust predictive efficacy. These findings align

Table 5

Multifactorial analysis of delta-insulin resistance versus pathological complete remission.

Indicators	*B*	SE	Wald	*P* value	OR	OR 95% CI	
						Lower	Upper
(a)							
dTC/HDL	0.868	0.369	5.551	**.018**	2.383	1.157	4.907
BMI	–0.913	0.596	2.349	.125	0.401	0.125	1.290
Hypertension	–0.646	0.192	11.286	**<.001**	0.524	0.359	0.764
Subtype	0.152	0.244	0.388	.533	1.164	0.722	1.877
dLDL	0.475	0.198	5.751	**.016**	1.608	1.091	2.370
(b)							
dTG/HDL	–0.098	0.097	1.007	.316	0.907	0.750	1.098
BMI	1.102	0.368	8.951	**.003**	3.011	1.462	6.197
Hypertension	–0.804	0.626	1.646	.200	0.448	0.131	1.528
Subtype	–0.700	0.201	12.134	**<.001**	0.496	0.335	0.736
dLDL	–0.508	0.394	1.662	.197	0.602	0.278	1.303
dTC	1.168	0.373	9.816	**.002**	3.216	1.549	6.677
(c)							
dTyG	–0.446	0.441	1.022	.312	0.640	0.270	1.519
BMI	1.100	0.370	8.834	**.003**	3.004	1.455	6.206
Hypertension	–0.874	0.640	1.866	.172	0.417	0.119	1.462
Subtype	–0.709	0.203	12.262	**<.001**	0.492	0.331	0.732
dLDL	–0.508	0.397	1.643	.200	0.601	0.276	1.309
dTC	1.199	0.385	9.714	**.002**	3.316	1.560	7.047
(d)							
dMetS-IR	2.726	1.283	4.514	**.034**	15.264	1.235	188.65
Hypertension	–0.796	0.601	1.755	.185	0.451	0.139	1.464
Subtype	–0.728	0.195	13.889	**<.001**	0.483	0.329	0.708
dLDL	–0.358	0.354	1.021	.312	0.699	0.349	1.400
dTC	1.110	0.342	10.506	**.001**	3.035	1.551	5.938

Bold value indicates statistically significant differences.

CI = confidence interval, FBG = fasting blood glucose, HDL-C = high-density lipoprotein cholesterol, LDL-C = low-density lipoprotein cholesterol, OR = odds ratio, TC = total cholesterol, TG = triglycerides, TyG = triglyceride glucose.

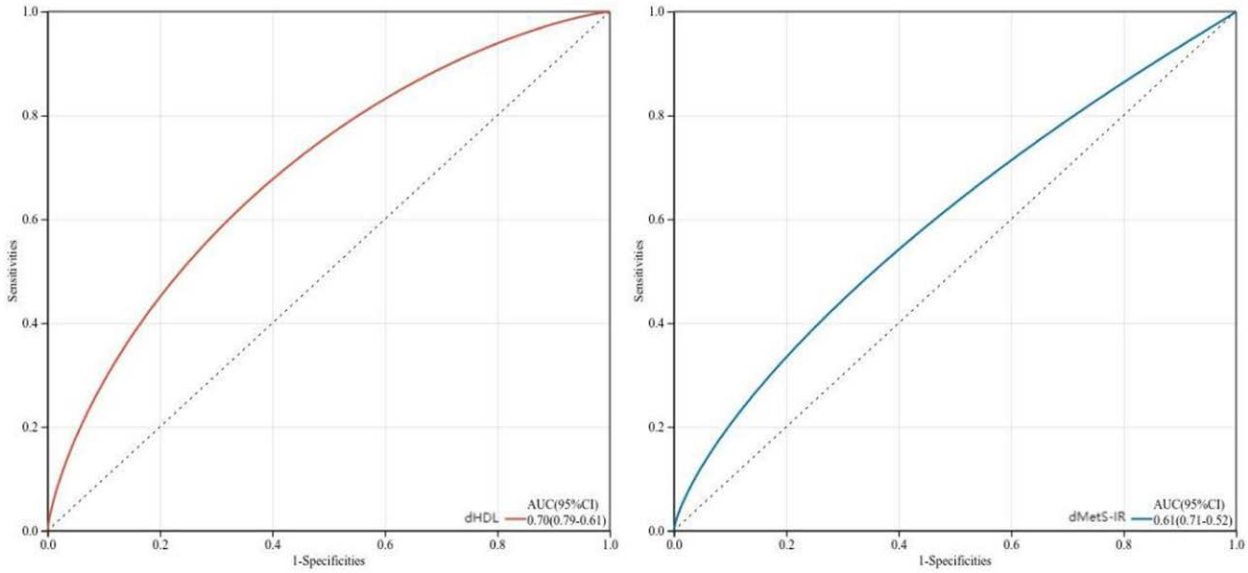

Figure 4. Clinical prediction modeling of ROC (dHDL AUC = 0.90, dMetS-IR = 0.61) with dTC/HDL and dMetS-IR. dMetS-IR = insulin resistance metabolic score following neoadjuvant chemotherapy, HDL-C = high-density lipoprotein cholesterol, ROC = receiver operating characteristic curve, TC = total cholesterol.

with the "metabolic adaptability" hypothesis proposed by Chen et al and Zhao et al,[17,18] wherein chemotherapeutic agents induce adaptive metabolic reprogramming in tumor cells, enabling survival within the tumor microenvironment (TME). Notably, tumor cells may propagate these metabolic signals via exosome-mediated communication to nonneoplastic TME components (e.g., cancer-associated fibroblasts), collectively reshaping metabolic features to establish a pro-tumorigenic niche. Static single-timepoint metrics used in prior studies fail to capture this dynamic interplay. Our results challenge Ruan et al's conclusions regarding the prognostic value of baseline metabolic parameters,[15] suggesting that dynamic IR monitoring may surpass single-timepoint assessments in clinical utility. Crucially, multivariate analysis confirmed the independence of ΔIR indices from confounding factors such as tumor subtype and hypertension, reinforcing their potential as standalone predictors. These discoveries introduce a novel metabolic dimension to therapeutic response prediction in breast cancer and advocate for a

paradigm shift from "static evaluation" to "dynamic monitoring" in future research.

We reveal a significant association between post-NAT metabolic deterioration (e.g., elevated TC/HDL ratio, increased MetS-IR) and reduced PCR rates, likely mediated by synergistic interactions across multiple biological pathways. First, aberrant activation of insulin/IGF-1 signaling may serve as a central mechanism.[19,20] While chemotherapy-induced ROS generation promotes tumor apoptosis during NAT, concurrent damage to pancreatic β-cells disrupts insulin secretion, triggering compensatory hyperinsulinemia.[21,22] Elevated insulin levels activate the IRS-1/PI3K-Akt-mTOR pathway, fostering tumor cell survival and proliferation,[23] while suppressing proapoptotic proteins (e.g., Bax, caspase-3) and upregulating antiapoptotic Bcl-2, thereby countering chemotherapy-induced apoptosis.[24] The observed inverse TC/HDL-PCR correlation (OR = 2.38) may reflect lipid metabolism-driven IRS-1 serine hyperphosphorylation,[25] which disrupts canonical insulin signaling and activates prosurvival pathways such as ER stress and c-Jun/JNK cascades, ultimately promoting tumor cell viability and growth.[26] Second, chronic inflammatory microenvironment remodeling may act as a critical mediator. IR-associated metabolic derangements (e.g., elevated TyG index) correlate with adipokine imbalance (increased leptin/adiponectin ratio)[27] and heightened IL-6/TNF-α levels.[28,29] These mediators may enrich chemotherapy-resistant tumor stem cells via STAT3[30]/NF-κB[31] pathways. The strong ΔIR-PCR association (OR = 15.26) suggests sustained inflammatory stimulation during treatment drives TME remodeling, though the lack of longitudinal serum inflammatory marker data limits mechanistic validation. Third, lipotoxicity-driven metabolic reprogramming warrants attention. Elevated TC/HDL ratios indicate impaired cholesterol efflux and oxidized LDL accumulation, potentially activating LOX-1 receptor-mediated ER stress.[32] Subsequent lipid/ERS axis activation (e.g., ApoB100 upregulation) induces autophagy, enabling tumor cells to eliminate damaged organelles and sustain energy production.[33] Preclinical evidence supports that multitarget interventions targeting cholesterol metabolism (e.g., LXRs agonists), ER stress (e.g., IRE1α inhibitors), and autophagy (e.g., chloroquine) may overcome therapeutic resistance.[34,35] While this study establishes dose–response relationships between metabolic indices and PCR, the absence of tumor tissue validation for cholesterol-related proteins (e.g., ABCA1, SCAP) confines mechanistic inferences to hypothetical constructs.

IR assessment relies on homeostatic model assessment of insulin resistance and oral glucose tolerance tests, yet their invasiveness and high costs limit clinical adoption. This study innovatively validates the potential of peripheral blood metabolic indices (e.g., TC/HDL ratio, TyG index) as IR surrogates for predicting NAT efficacy in breast cancer. Our findings not only methodologically complement the metformin intervention mechanisms proposed by the METTEN[36] and METEOR[37] studies but also pioneer the development of a predictive model based on routine clinical parameters (TC/HDL AUC = 0.7). This model provides primary care institutions with an operationally feasible tool for therapeutic response assessment, addressing the unmet need for cost-effective prognostic strategies in resource-limited settings.

Metabolic modulation emerges as a promising therapeutic frontier. Preclinical studies demonstrate that metformin synergizes with anticancer therapies to suppress cell proliferation, colony formation, migration, and invasion. Notably, in ex ovo chorioallantoic membrane (CAM) models, metformin significantly reduces tumor volume and metastatic potential.[38] A phase III trial further suggests metformin may ameliorate diabetes- and insulin therapy-associated adverse prognoses.[39] Mechanistically, metformin attenuates leptin signaling, thereby suppressing JAK2-STAT3 and PI3K-Akt-mTOR pathways in cancer cells.[20] Additionally, PPARγ antagonists (e.g., GW9662) show preclinical efficacy in reversing lipid metabolism-associated drug resistance by improving insulin sensitivity,[40] suggesting that combined targeting of metabolic pathways may represent a promising therapeutic strategy.

This study has the following limitations. First, single-center retrospective design risks selection bias. Second, insufficient sample size (N = 132) for subtype analyses. Finally, short-term follow-up lacks survival correlation. Priorities involve: establishing multicenter cohorts with serial metabolomics during NAT, developing artificial intelligence models integrating metabolic-radiomic patterns, and investigating metabolic priming windows through adaptive trial designs. These strategies address current evidence gaps while optimizing predictive accuracy and therapeutic synergy between metabolic interventions and conventional chemotherapy.

5. Conclusion

Dynamic monitoring of TC/HDL and MetS-IR predicts PCR in NAT, with elevated levels inversely correlating to PCR rates. These cost-effective biomarkers justify clinical metabolic surveillance, implying chemotherapy-induced lipid dysregulation management could optimize outcomes. Multicenter validation of prognostic thresholds and metabolic reprogramming-based combination therapies warrant prioritized investigation.

Author contributions

Conceptualization: Yi Zeng.
Data curation: Yi Zeng.
Formal analysis: Yi Zeng.
Methodology: Yi Zeng.
Resources: Yi Zeng.
Supervision: Yi Zeng.
Validation: Yi Zeng.
Writing – original draft: Yi Zeng.
Writing – review & editing: Yi Zeng.

References

[1] Bray F, Laversanne M, Sung H, et al. Global cancer statistics 2022: GLOBOCAN estimates of incidence and mortality worldwide for 36 cancers in 185 countries. CA Cancer J Clin. 2024;74:229–63.
[2] Fisher B, Brown A, Mamounas E, et al. Effect of preoperative chemotherapy on local-regional disease in women with operable breast cancer: findings from National Surgical Adjuvant Breast and Bowel Project B-18. J Clin Oncol. 1997;15:2483–93.
[3] Early Breast Cancer Trialists' Collaborative Group (EBCTCG). Long-term outcomes for neoadjuvant versus adjuvant chemotherapy in early breast cancer: meta-analysis of individual patient data from ten randomised trials. Lancet Oncol. 2018;19:27–39.
[4] Bear HD, Anderson S, Brown A, et al; National Surgical Adjuvant Breast and Bowel Project Protocol B-27. The effect on tumor response of adding sequential preoperative docetaxel to preoperative doxorubicin and cyclophosphamide: preliminary results from National Surgical Adjuvant Breast and Bowel Project B-27. J Clin Oncol. 2003;21:4165–74.
[5] Fisher B, Bryant J, Wolmark N, et al. Effect of preoperative chemotherapy on the outcome of women with operable breast cancer. J Clin Oncol. 2023;41:1795–808.
[6] Bear HD, Anderson S, Smith RE, et al. Sequential preoperative or postoperative docetaxel added to preoperative doxorubicin plus cyclophosphamide for operable breast cancer: National Surgical Adjuvant Breast and Bowel Project Protocol B-27. J Clin Oncol. 2006;24:2019–27.
[7] Rastogi P, Anderson SJ, Bear HD, et al. Preoperative chemotherapy: updates of National Surgical Adjuvant Breast and Bowel Project Protocols B-18 and B-27. J Clin Oncol. 2008;26:778–85.
[8] Cortazar P, Zhang L, Untch M, et al. Pathological complete response and long-term clinical benefit in breast cancer: the CTNeoBC pooled analysis. Lancet. 2014;384:164–72.
[9] Szablewski L. Insulin resistance: the increased risk of cancers. Curr Oncol. 2024;31:998–1027.

[10] Tong YW, Wang G, Wu JY, et al. Insulin-like growth factor-1, metabolic abnormalities, and pathological complete remission rate in HER2-positive breast cancer patients receiving neoadjuvant therapy. Onco Targets Ther. 2019;12:3977–89.
[11] Zhou Z, Zhang Y, Li Y, et al. Metabolic syndrome is a risk factor for breast cancer patients receiving neoadjuvant chemotherapy: a case-control study. Front Oncol. 2023;12:1080054.
[12] Kheirollahi A, Teimouri M, Karimi M, et al. Evaluation of lipid ratios and triglyceride-glucose index as risk markers of insulin resistance in Iranian polycystic ovary syndrome women. Lipids Health Dis. 2020;19:235.
[13] Zhou M, Zhu L, Cui X, et al. The triglyceride to high-density lipoprotein cholesterol (TG/HDL-C) ratio as a predictor of insulin resistance but not of beta cell function in a Chinese population with different glucose tolerance status. Lipids Health Dis. 2016;15:104.
[14] Bello-Chavolla OY, Almeda-Valdes P, Gomez-Velasco D, et al. METS-IR, a novel score to evaluate insulin sensitivity, is predictive of visceral adiposity and incident type 2 diabetes. Eur J Endocrinol. 2018;178:533–44.
[15] Ruan GT, Xie HL, Hu CL, et al. Comprehensive prognostic effects of systemic inflammation and insulin resistance in women with breast cancer with different BMI: a prospective multicenter cohort. Sci Rep. 2023;13:4303.
[16] Wu X, Wang S, Lin L, et al. Association between triglyceride glucose index and breast cancer in 142,184 Chinese adults: findings from the REACTION study. Front Endocrinol (Lausanne). 2024;15:1321622.
[17] Chen X, Kuang S, He Y, et al. The differential metabolic response of oral squamous cell carcinoma cells and normal oral epithelial cells to cisplatin exposure. Metabolites. 2022;12:389.
[18] Zhao C, Liu S, Gao F, Zou Y, Ren Z, Yu Z. The role of tumor microenvironment reprogramming in primary liver cancer chemotherapy resistance. Front Oncol. 2022;12:1008902.
[19] Hauner D, Hauner H. Metabolic syndrome and breast cancer: is there a link? Breast Care (Basel). 2014;9:277–81.
[20] Khandekar MJ, Cohen P, Spiegelman BM. Molecular mechanisms of cancer development in obesity. Nat Rev Cancer. 2011;11:886–95.
[21] Chiang FF, Huang SC, Yu PT, Chao TH, Huang YC. Oxidative stress induced by chemotherapy: evaluation of glutathione and its related antioxidant enzyme dynamics in patients with colorectal cancer. Nutrients. 2023;15:5104.
[22] Basu L, Grieco-St-Pierre L, Ching MEA, et al. Cisplatin exposure dysregulates insulin secretion in male and female mice. Diabetes. 2025;74:528–43.
[23] Ye L, Liu X, Jin K, et al. Effects of insulin on proliferation, apoptosis, and ferroptosis in primordial germ cells via PI3K-AKT-mTOR signaling pathway. Genes (Basel). 2023;14:1975.
[24] Zhong Z, Wang T, Zang R, et al. Dual PI3K/mTOR inhibitor PF-04979064 regulates tumor growth in gastric cancer and enhances drug sensitivity of gastric cancer cells to 5-FU. Biomed Pharmacother. 2024;170:116086.
[25] Ghoshal K, Luther JM, Pakala SB, et al. Epoxygenase Cyp2c44 regulates hepatic lipid metabolism and insulin signaling by controlling FATP2 localization and activation of the DAG/PKCδ axis. Diabetes. 2024;73:1229–43.
[26] AlBashtawi J, Al-Jaber H, Ahmed S, Al-Mansoori L. Impact of obesity-related endoplasmic reticulum stress on cancer and associated molecular targets. Biomedicines. 2024;12:793.
[27] Naimo GD, Forestiero M, Giordano F, et al. Adiponectin influences the behavior of stem cells in hormone-resistant breast cancer. Cells. 2025;14:286.
[28] Vasiyani H, Mane M, Rana K, et al. DNA damage induces STING mediated IL-6-STAT3 survival pathway in triple-negative breast cancer cells and decreased survival of breast cancer patients. Apoptosis. 2022;27:961–78.
[29] Bunnell BA, Martin EC, Matossian MD, et al. The effect of obesity on adipose-derived stromal cells and adipose tissue and their impact on cancer. Cancer Metastasis Rev. 2022;41:549–73.
[30] Wu L, Ge Y, Yuan Y, et al. Genome-wide CRISPR screen identifies MTA3 as an inducer of gemcitabine resistance in pancreatic ductal adenocarcinoma. Cancer Lett. 2022;548:215864.
[31] Lin JF, Liu ZX, Chen DL, et al. Nucleus-translocated GCLM promotes chemoresistance in colorectal cancer through a moonlighting function. Nat Commun. 2025;16:263.
[32] Jiang G, Li J, Niu S, Dong R, Chen Y, Bi W. LY86 facilitates ox-LDL-induced lipid accumulation in macrophages by upregulating SREBP2/HMGCR expression. BMC Cardiovasc Disord. 2024;24:289.
[33] Yin ZY, He SM, Zhang XY, et al. Apolipoprotein B100 acts as a tumor suppressor in ovarian cancer via lipid/ER stress axis-induced blockade of autophagy. Acta Pharmacol Sin. 2025;46:1445–1461.
[34] Taank Y, Randhawa V, Agnihotri N. Ergosterol and its metabolites as agonists of liver X receptor and their anticancer potential in colorectal cancer. J Steroid Biochem Mol Biol. 2024;243:106572.
[35] Alam R, Kabir MF, Kim HR, Chae HJ. Canonical and noncanonical ER stress-mediated autophagy is a bite the bullet in view of cancer therapy. Cells. 2022;11:3773.
[36] Martin-Castillo B, Pernas S, Dorca J, et al. A phase 2 trial of neoadjuvant metformin in combination with trastuzumab and chemotherapy in women with early HER2-positive breast cancer: the METTEN study. Oncotarget. 2018;9:35687–704.
[37] Kim J, Lim W, Kim EK, et al. Phase II randomized trial of neoadjuvant metformin plus letrozole versus placebo plus letrozole for estrogen receptor positive postmenopausal breast cancer (METEOR). BMC Cancer. 2014;14:170.
[38] Mahmoudi G, Ehteshaminia Y, Kokhaei P, et al. Enhancement of targeted therapy in combination with metformin on human breast cancer cell lines. Cell Commun Signal. 2024;22:10.
[39] Sonnenblick A, Agbor-Tarh D, Bradbury I, et al. Impact of diabetes, insulin, and metformin use on the outcome of patients with human epidermal growth factor receptor 2-positive primary breast cancer: analysis from the ALTTO Phase III Randomized Trial. J Clin Oncol. 2017;35:1421–9.
[40] Chen S, Liu Z, Wu H, et al. Adipocyte-rich microenvironment promotes chemoresistance via upregulation of peroxisome proliferator-activated receptor gamma/ABCG2 in epithelial ovarian cancer. Int J Mol Med. 2024;53:37.